2013 IEEE 10th International Symposium on Biomedical Imaging:
From Nano to Macro
San Francisco, CA, USA, April 7-11, 2013

# AUTOMATED SPATIAL ANALYSIS OF ARK2: PUTATIVE LINK BETWEEN MICROTUBULES AND CELL POLARITY

*G. Harlow*[1], *A. C. Cruz*[2], *S. Li*[1], *N. S. Thakoor*[2], *A. C. Bianchi*[2], *J. Chen*[1], *B. Bhanu*[2] *and Z. Yang*[1]

[1]Department of Botany and Plant Sciences, University of California, Riverside, CA, 92521
[2]Center for Research in Intelligent Systems, University of California, Riverside, CA, 92521

## ABSTRACT

In leaves of *A. thaliana*, there exists an intricate network of epidermal surface layer cells responsible for anatomical stability and vigor of flexibility to the entire leaf. Rho GTPases direct this organization of cell polarity, but full understanding of the underlying mechanisms demands further inquiry. We conduct two experiments: (1) a novel procedure is proposed that could be used in other life and plant science studies to quantify microtubule orientation, and (2) shape analysis. We hypothesize ARK2 as a putative interactor in cell polarity maintenance through stabilization of microtubule ordering. We are the first to automate pavement cell phenotype analysis for cell polarity and microtubule orientation. Breakthroughs in the signaling network regulating leaf cell polarity and development will lead science into the frontier of genetically modifying leaves to dramatically increase Earth's plant biomass; impending food shortages in the 21st century will be well served by such research.

***Index Terms***— Image texture analysis, image shape analysis, microtubulues, ROP GTPase signaling, cell polarity

## 1. INTRODUCTION

Leaves are the fundamental basis for human life on earth. They require an intricate pattern of interlocking cells on their epidermal surface layer to maintain structural integrity and tensile strength. All plant structures can be derived from leaves under the appropriate hormonal and transcription factor conditions. Shape, polarity, and pattern formation are centrally important to explaining the cardinal rules governing polar structure development in living organisms. In *A. thaliana*, the adaxial epidermal surface layer of cells are called pavement cells. They interdigitate like puzzle pieces, producing a flat leaf surface. Each cell is composed of lobes and indentations in a flat plane, see Figure 1. ROP GTPases direct the growth of these lobes and indentations with a series of downstream effectors [1]. ROP6 and RIC1 coordinate the parallel planar ordering of microtubules between directly opposite indentations [2]. The formation of lobes is directed by

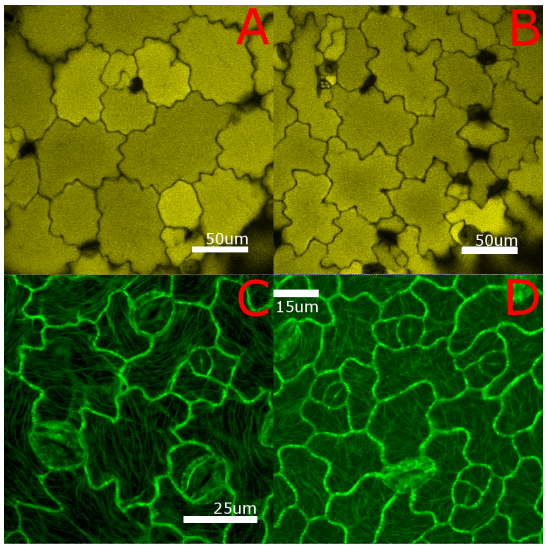


**Fig. 1**. Sample images. (Top) Transient light image of pavement cells of (A) ark2-1 and (B) WT. (Bottom) GFP-tagged pavement cells of (C) ark2-1 and (D) WT.

ROP2 and ROP4 [3]. These ROPs act through RIC4 which induces F-actin accumulation in lobes, scaffolding outward lobe protuberances [3]. Previous state-of-the-art work in pavement cells used manual analysis to compare phenotypes [1, 2]. A small number of experts would extract shape characteristics of pavement cell lobes by hand.

We contribute the following: (A) to the best of our knowledge, we are the first paper to completely automate pavement cell phenotype analysis for cell polarity and microtubule orientation. (B) We investigate the present cell polarity signaling model to further elucidate the network of proteins [1] governing the mechanics of cell shape development in pavement cells. We anticipate that ARK2 is the key protein linking microtubule ordering with cell polarity formation. (C) We propose a novel procedure for quantifying microtubule ordering which can be applied to microtubule or F-actin analysis, as well as in other plant science and life science assays.

## 2. METHODS

Individual lines of EMS-mutated ROP6-overexpression mutants underwent a genetic screen to identify enhanced pheno-

**Acknowlegements**: Support for this work was provided for in part by NSF grant 0727129, NSF IGERT: Video Bioinformatics Grant DGE 0903667 and NIH grant R01GM081451. The contents and information do not reflect the position or policy of the U.S. Government.

types and to examine the underlying genes controlling pavement cell shape. Map-based cloning identified genetic origin. From this, the gene ARK2 was identified, mutated from the EMS treatment through modification of an individual nucleotide in the kinesin motor domain. This new ARK2 mutant line (ark2-1) was then crossed with GFP-TUA, allowing for the visualization of microtubule ordering using microscopy. Given its hypothesized effect on root hair polarity [6], ARK2 is the primary focus of our study lending to the shared overlap between many cell polarity signaling cascades.

### 2.1. Data Acquisition

All images were captured using the Leica SP2. Cell morphology images were taken using transient light (Figure 1-A, B). GFP labeled microtubule ordering was taken using 488nm light at 60% strength (Figure 1-C, D). Plant samples were grown in sunshine LC1 mix soil under daily 16 hour light, 8 hour dark fluorescent bulb cycles. Images were taken from 18 day old plants exhibiting their third true leaves. Cell ROI is detected on a per-image basis with the following schema. Let be $I$ an image: (1) intensity values are normalized with a contrast adjustment. (2) $I$ is denoised with a Gaussian filter of variance $\sigma$. (3) $I$ is morphologically opened with a disk-shaped structuring element of size $L$; this separates cell ROI that is joined because of a weakly fluorescing cell membrane. (4) The cells are segmented with a probabilistic framework that models pixel intensity as a mixture model [4]. The segmented, connected regions are each taken to be a cell.

### 2.2. Microtubule Analysis

Microtubule controls the development of a cell's shape and structure. It is important to identify any changes a mutant may have on microtubule structure. For this experiment, GFP-TUA was crossed with mutant ark2-1 and compared with wild type GFP-TUA lines to investigate microtubule arrangement. This allowed the visualization of ark2-1's influence on the internal structural dynamics of pavement cell development. An example of the microtubule data is given in Figure 2. Note that there is an underlying background texture. We want to isolate only the edges belonging to the microtubule. The novel procedure for quantifying their orientation is as follows: (A) We suppress background texture with isotropic texture inhibition. Let $E_{\theta_i}(x,y)$ be the Gabor energy at orientation $\theta_i$, where $(x,y)$ is the location. An energy map $\hat{E}$ that captures the highest energy across all orientations is constructed for each pixel:

$$\hat{E}(x,y) = \max\left\{E_\theta(x,y)\,|\theta = \theta_1, ..., \theta_N\right\} \quad (1)$$

Separately, an orientation map is constructed that contains the dominant orientation for each pixel:

$$\Theta(x,y) = \text{argmax}_\theta\left\{E_\theta(x,y)\,|\theta = \theta_1, ..., \theta_N\right\} \quad (2)$$

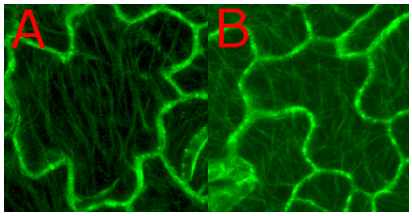


**Fig. 2**. Ark2-1's effect on microtubule direction. Ark2-1 microtubules tend to have similar orientation (A), unlike wild type (B).

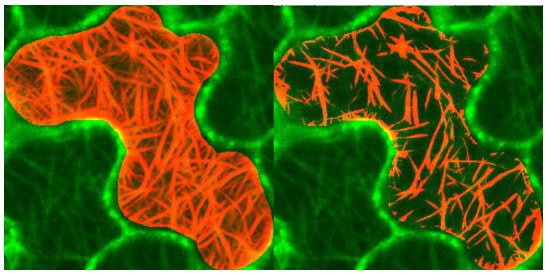

**Fig. 3**. Microtubule detection from the cell in Figure 2. (Left) Dominant edges from Eq. 5 captured with a Gabor filter and superimposed on the image in red and (Right) the same edges with a nonclassical receptive field.

The inhibition term, which measures the background texture to be suppressed, is:

$$t(x,y) = \left(\hat{E} * w\right)(x,y) \quad (3)$$

where $w$ is a weight function:

$$w(x,y) = \frac{1}{\|g(\text{DoG})\|_1} g(\text{DoG}(x,y)) \quad (4)$$

where DoG is a Difference of Gaussians and $g(z) = H(Z) * z$, where $H$ is a Heaviside step function. Finally, the non-CRF is computed as:

$$b(x,y) = g\left(\hat{E}(x,y) - \alpha t(x,y)\right) \quad (5)$$

where $\alpha$ controls the strength of texture suppression. The effect of a nonclassical receptive field is given in Figure 3. This process is also referred to as isotropic inhibition [5].

(B) Eq. 5 gives the isolated edges. We want to find the distribution of orientations; this is done by examining the histogram. After computing the non-CRF response, the edges within each cell are aggregated with a soft histogram:

$$h(\theta_i) = \sum_{\forall(x,y)|\Theta(x,y)=\theta_i} b(x,y) \quad (6)$$

(C) If all the microtubule orientations are similar, the histogram of should be normally distributed. A normal distribution is estimated with maximum likelihood. Then, the quality of fit is measured with excess kurtosis: $\mu_4/\sigma_4 - 3.$ , where $\mu_4$ is the fourth moment about the mean and $\sigma_4$ is the squared variance.

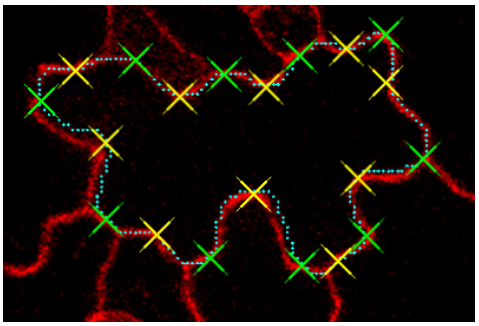

**Fig. 4**. A pavement stained with propidium iodide with super-imposed curvature (cyan dotted line), concave inflection points (yellow crosses) and convex inflection points (green crosses).

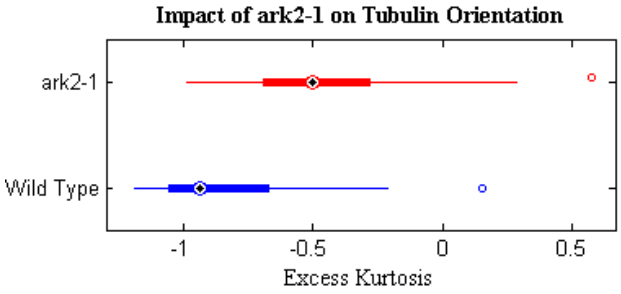


**Fig. 5**. Excess kurtosis for (top) ark2-1 and (bottom) wild type. Microtubule direction in ark2-1 tends to be more directed (excess kurtosis value closer to 0 than the wild type).

*2.2.1. Microtubule Analysis*

Morphological properties of pavement cell lobes, indentations, and total cell shape are the natural consequence of the underlying cell polarity mechanisms dictated by ROP signaling and its downstream effectors. Quantifying cell polarity in this manner can reveal to us the measureable effect of each gene on pavement cell patterning.

Conventional, manual analysis methods would analyze only the shape attributes of the lobes within each cell. For our morphological analysis, this plus the shape attributes of the cell as a whole. After cell ROI extraction, individual cells are identified with a 4-connected nearest neighbor. The boundary of each cell is refined by estimating curvature with a multiscale Fourier transform-based approach [6]. The reader is referred to Figure 4. We define a lobe as a triplet of inflection points: the edges of the lobe are convex inflection points, and the peak, or middle of the lobe is a concave inflection point.

For each cell, we measure the solidity; extent; perimeter; Hu moments 1, 2 and 8; the mean lobe height, width and area (approximated as the triangle between the three points defining the lobe) of all the lobes in the cell; lobe count; lobe to area ratio and circularity.

## 3. RESULTS AND DISCUSSION

From initial inspection of ark2-1 there was an ordering of microtubules that was close to parallel. Observable effects of ARK2 mutation were disruption of native diffuse microtubule organization, and distorted cell morphology, compared to the wild type. The system parameters are as follows: $\sigma = 3$, $l = 3$, $\alpha = 1$, to suppress all background texture; $N = 32$, spaced evenly such that $\theta_{N+1} = \pi$. These parameters are empirically selected to best replicate groundtruth values that had been manually extracted by three expert manual segmentations. For microtubule analysis, 99 cells are analyzed; shape attribute analysis. Significance of the results is determined with a Welsh's t-test. For all figures, wild type indicates A. thaliana Col-0.

The impact of ark2-1 on microtubule direction is given in Figure 5. The left and right boundaries indicate the upper/lower 25/75th percentile boundaries. The whiskers extend to twice the standard deviation. Circles are outliers. The black circle with a dot in the middle indicates the median value. Excess kurtosis measures skewness and can be interpreted as distance from a normal distribution. -1.2 implies uniformly oriented microtubule direction, whereas a value closer to 0 implies a perfect normal distribution. The t-test value for this experiment is 0.005; this is statistically significant. It can be stated that microtubule orientation in ark2-1 is more parallel than in the wild type. We posit that the reason for this result is that ARK2-1 acts as a motor protein on microtubules. We believe the mutation of the 312th amino acid of the kinesin domain from serine to phenylalanine of ark2-1 has conferred a gain of function trait to ark2-1. This has resulted in increased microtubule ordering which can be visually confirmed in Figure 1A.

The impact of ark2-1 on shape attributes is given in Table 1.The first Hu moment and the solidity are significant across all molarities. Solidity measures the proportion of pixels that are contained in the convex area of the cell. From Figure **??**, it can be observed that ark2-1 is more circular, versus the wild type, which has branches not located in the convex hull enclosing the shape. This results in very distinct shape between ark2-1 and the wild type, leading to the 1st Hu moment being a discriminating descriptor between the two groups. A box plot is given in Figure 6 comparing the first Hu moment and the solidity. Hypothesizing that ARK2 is involved as the link between NEK6 and microtubules, it was expected and observed that disruption of ARK2 would result in increased solidity. Without the dynamic variable ordering as seen in wild type, the development and maintenance of stability in lobes was restricted and disrupted. The increased microtubule ordering acts to reduce the expansibility of the total cell, preventing native lobe formation.

Lobes have historically been identified as outgrowths or localized lateral expansion from their anticlinal walls into adjacent cells [1]. A more objective classification for a lobe was required, and we define them as three adjacent inflection points along the curvature of the lobe; this may differ from the conventional definition of a lobe [3, 1, 7]. However, because our method is principled and automated, it was able to detect

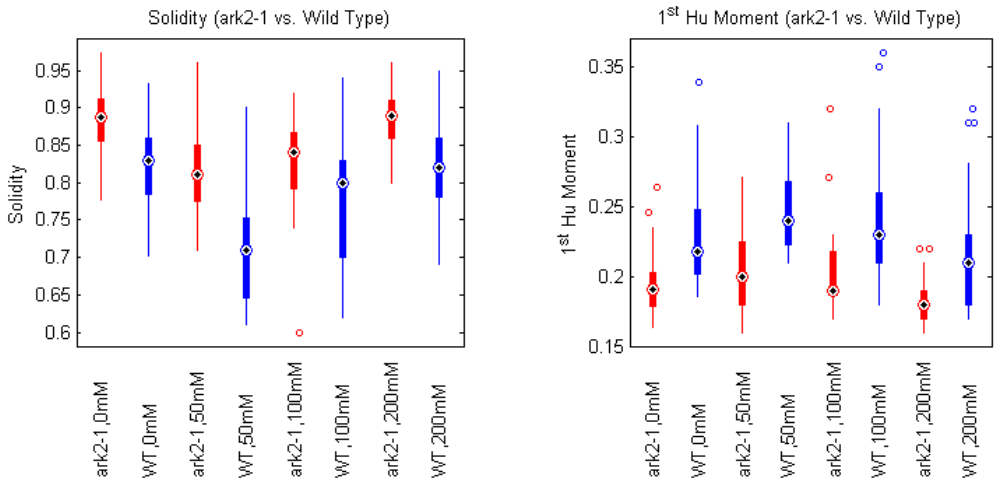


**Fig. 6**. Comparison (a) 1st Hu moment and (b) solidity for species 37 and wild type for molarities of 50mM, 100mM and 200mM.

**Table 1**. Student's t-test values for shape attributes (ark2-1 vs. WT)

| Attribute Name | 0mM | 50mM | 100mM | 200mM |
|---|---|---|---|---|
| Solidity | **.0000** | **.0000** | **.0016** | **.0000** |
| Extent | **.0018** | **.0000** | .0552 | **.0000** |
| Perimeter | .4643 | **.0008** | .2129 | .4472 |
| Hu Moment 1 | **.0006** | **.0000** | **.0001** | **.0000** |
| Hu Moment 2 | .0801 | **.0254** | .0582 | .0604 |
| Hu Moment 8 | .1835 | **.0070** | .0522 | .1021 |
| Mean Lobe Height | .4368 | **.0013** | .2239 | .4339 |
| Mean Lobe Width | .5174 | **.0003** | .2355 | .2166 |
| Mean Lobe T. Area | .2692 | **.0028** | .1209 | .1055 |
| Lobe Count | .9549 | **.0020** | .1209 | .1021 |
| Lobe/Area Ratio | .1753 | **.0007** | .0373 | .8165 |
| Circularity | **.0001** | **.0000** | .0909 | **.0216** |

small, budding lobes that manual analysis might otherwise miss. This high throughput tool enhanced lobe detectability, accuracy of measure, and clarity and objectivity of conclusions.

## 4. CONCLUSION

Through initial visual screening a mutant with rounder cells and reduced lobes was discovered. After MAP-based cloning the locus of the gene was identified as AT1G01950 (ARK2) and exhibited a single point mutation in the third codon of the 312th amino acid converting a native cytosine to thymine. This caused a mutation in the kinesin domain of ARK2 via serine now being expressed as phenylalanine. Due to the limited objectivity in previous studies, this paper developed a new tool specifically suited to characterize and quantify the physiological consequences of this mutant which revealed several key findings. Ark2-1 dramatically increases microtubule ordering, thus restricting cell expansibility. Additionally, ark2-1 exhibits reduced lobe number and a higher degree of circularity. We hypothesize this relationship is dictated by intermediaries in microtubule ordering given the interaction between ARK2 and NEK6 [6], and ARK2 is a key protein in cell polarity maintenance and pavement cell shape. Future work will incorporate interaction studies between the putative molecular species hypothesized herein as well as actin quantification studies to further illuminate ARK2s role in lobe development.

## 5. REFERENCES

[1] Y. Fu et al., "Arabidopsis interdigitating cell growth requires two antagonistic pathways with opposing action on cell morphogenesis," *Cell*, vol. 120, no. 5, pp. 687 – 700, 2005.

[2] T. Xu et al., "Cell surface and rho gtpase-based auxin signaling controls cellular interdigitation in arabidopsis," *Cell*, vol. 143, no. 1, pp. 99 – 110, 2010.

[3] Y. Fu et al., "The rop2 gtpase controls the formation of cortical fine f-actin and the early phase of directional cell expansion during arabidopsis organogenesis," *The Plant Cell*, vol. 14, no. 4, pp. 777 – 794, 2002.

[4] S. Sopinath et al., "A statistical approach for intensity loss compensation of confocal microscopy images," *J. Microscopy*, vol. 230, no. 1, pp. 143 – 159, 2008.

[5] C. Grigorescu et al., "Contour detection based on nonclassical receptive field inhibition," *IEEE Trans. IP*, vol. 12, no. 7, pp. 729 – 739, 2003.

[6] J.-P. Antoine et al., "Shape characterization with the wavelet transform," *Signal Processing*, vol. 62, no. 3, pp. 265 – 290, 1997.

[7] T. Sakai et al., "Armadillo repeat-containing kinesins and a nima-related kinase are required for epidermal-cell morphogenesis in arabidopsis," *Plant J.*, vol. 53, no. 1, pp. 2007, 2008.